

A conserved higher-order anisotropic traffic flow model: Description of equilibrium and non-equilibrium flows

Peng Zhang^a, S.C. Wong^{b,*}, S.Q. Dai^a

^a Shanghai Institute of Applied Mathematics and Mechanics, Shanghai University, China

^b Department of Civil Engineering, The University of Hong Kong, Hong Kong SAR, China

ARTICLE INFO

Article history:

Received 19 June 2007

Received in revised form 17 March 2008

Accepted 18 October 2008

Keywords:

Hyperbolic conservation laws

Physically bounded solution

Unstable equilibrium

Stop-and-go waves

ABSTRACT

This paper takes into account three regimes for the description of traffic dynamics, which include the introduction of a pseudo-density transformed from the velocity, the pressure as a function of the pseudo-density and the relaxation of velocity to equilibrium. The resultant characteristic variables can be used to measure the deviation of the phase state to a desired state and derive physically bounded solutions. Taking the pseudo-density as a conserved variable, the approach is able to describe both equilibrium and non-equilibrium flows in a systematic and unified manner, and thus complex traffic phenomena. The theoretical properties of the model are thoroughly investigated, and numerical examples are used to demonstrate the ability of the model to reproduce some notable traffic phenomena.

© 2008 Elsevier Ltd. All rights reserved.

1. Introduction

In this research we index three developments in continuum traffic flow models. The first is the exposition of the LWR theory by Lighthill and Whitham (1955), and independently by Richards (1956). The second, which is ascribed to Payne (1971) and Whitham (1974), is the description of traffic acceleration equations. These are known as PW-type models, and due to their extensive use by many researchers have dominated the field for decades. The third is the severe critique of the PW-type models by Daganzo (1995) and the proposal of a new model by Aw and Rascle (2000) that reveals the *anisotropic* nature of traffic flows. Similar research was also carried out by Zhang (2002), Jiang et al. (2002), Xue and Dai (2003), and more recently by Lebacque et al. (2007a,b). The evolution of these three types of models is briefly described as follows.

The LWR theory models traffic movements as a continuous flow with a density ρ , an average velocity v , and a flow $q = \rho v$, which are functions of location x and time t . As in fluid dynamics, the mass conservation reads as follows:

$$\partial_t \rho + \partial_x(\rho v) = 0, \quad (1)$$

where for simplicity, the on-and-off ramp flows are not considered. The model is completed by the following equation. By assuming the velocity–density relationship

$$v = v_e(\rho),$$

the LWR model is then acquired as the scalar conservation equation

$$\partial_t \rho + \partial_x(\rho v_e(\rho)) = 0. \quad (2)$$

* Corresponding author. Tel.: +852 2859 1964; fax: +852 2559 5337.

E-mail addresses: pengzhang@ustc.edu (P. Zhang), hhecwsc@hkucc.hku.hk (S.C. Wong), sqdai@guomai.sh.cn (S.Q. Dai).

Here, $v_e(\rho)$ is strictly decreasing in $\rho \in [0, \rho_{\text{jam}}]$ where ρ_{jam} is the jam density, and the maximum and minimum velocities are $v_e(0) \equiv v_f$ and $v_e(\rho_{\text{jam}}) = 0$, respectively.

Let $q_e(\rho) \equiv \rho v_e(\rho)$. If $q_e''(\rho) < 0$, then the LWR model is analogous to the Burgers equation, and is thus characterized by nonlinear waves known as shocks and rarefactions (Whitham, 1974; Smoller, 1983; Toro, 1999; LeVeque, 2002). These shocks or rarefactions arise from an increase or decrease in density downstream.

The LWR model is considered to be inadequate for the modeling of traffic dynamics, as the phase plot of the velocity and density is merely a fixed (equilibrium) curve. To overcome this problem, the PW-type models were proposed as 2×2 systems (Payne, 1971; Whitham, 1974; Kühne, 1984; Kerner and Konhäuser, 1994) in which the acceleration equations take the same form

$$\partial_t v + v \partial_x v = \frac{v_e(\rho) - v}{\tau} - \frac{c^2(\rho)}{\rho} \partial_x \rho + v \partial_x^2 v. \quad (3)$$

The left-hand side of the equation is the traffic acceleration $d\nu/dt \equiv \partial_t v + v \partial_x v$, the first term on the right-hand side models the relaxation to the equilibrium state $(\rho, v_e(\rho))$ in the $\rho - v$ coordinate frame, and the remaining terms describe the anticipation of the surroundings. Although the PW model (Payne, 1971; Whitham, 1974) is able to reproduce many observed phenomena, such as stop-and-go waves, it was criticized by Daganzo (1995) for its isotropic nature, which results from the wave propagation being faster than the traffic movement and gives rise to reverse flows (wrong-way traffic) in many cases. The two characteristic speeds of Eqs. (1) and (3) are denoted as $\lambda_{1,2} = v \mp c$.

To “repair” the PW-type models, Aw and Rascle (2000) introduced a “pressure” term $p = p(\rho)$, $p'(\rho) > 0$, in which the acceleration is determined by the convective derivative of $p(\rho)$, namely

$$\partial_t v + v \partial_x v = -(\partial_t p(\rho) + v \partial_x p(\rho)). \quad (4)$$

This is different from the PW-type models, in which the anticipation is the partial derivative $-\partial_x p(\rho)$ with a sound velocity $c(\rho) = \rho p'(\rho)$. By applying Eq. (1), Eq. (4) can be simplified to

$$\partial_t v + (v - \rho p'(\rho)) \partial_x v = 0. \quad (5)$$

The two characteristic speeds of Eqs. (1) and (5) can be easily solved as $\lambda_1 = v - \rho p'(\rho)$ and $\lambda_2 = v$, which are no greater than the traffic speed. In other words, the movement of a vehicle is not influenced by vehicles upstream and there is no incidence of reverse flow, which means that the drawbacks of the PW-type models are overcome. A similar discussion is given in Zhang (2002), Jiang et al. (2002), and Xue and Dai (2003), with $p'(\rho) = -v'_e(\rho)$, $1/\rho$, and $-t_r v'_e(\rho)/T(\rho)$ in Eq. (5), respectively. In these three models and subsequent studies by Rascle (2002), Greenberg (2004) and Lebacque et al. (2007a), the relaxation term is taken into account. The following are some remarks on all of these models.

In addition to the mass conservation, which is physically meaningful, it is necessary to define another conservation form for mathematical reasons. If this is not undertaken, then the definition of weak solutions is ambiguous in their description of the discontinuities, and it becomes difficult to interpret the resultant traffic waves, such as shocks. The numerical scheme should also be conserved, and should be based upon defined conservation equations. However, this issue is not well addressed in the literature, except in a recent study by Aw and Rascle (2000) (see also Zhang et al., 2005; Zhang and Wong, 2006). In Aw and Rascle (2000), the required conservation form was defined as

$$\partial_t(\rho(v + p(\rho))) + \partial_x(\rho v(v + p(\rho))) = 0, \quad (6)$$

which is obtained by multiplying Eq. (1) with $v + p(\rho)$ and Eq. (4) with ρ and adding the two together (see also Rascle, 2002). Here, the function $\rho(v + p(\rho))$ is taken as the conserved variable. The conservation form of the acceleration equations in Zhang (2002), Jiang et al. (2002), and Xue and Dai (2003) can take the same form of Eq. (6). For the isotropic models that are represented by Eq. (3), we mentioned in Zhang and Wong (2006) that either the velocity v or the flow $q = \rho v$ can be taken as the conserved variables. More recently, Lebacque et al. (2007b) replaced $v + p(\rho)$ with I in Eq. (6). This gives, with the relaxation term

$$\partial_t(\rho I) + \partial_x(\rho v I) = \frac{q_e - q}{\tau}. \quad (7)$$

Here, I was explained as a more general variable that is related to the driver's attribute.

For anisotropic models, there are different possible choices for the pressure $p(\rho)$ and equilibrium velocity $v_e(\rho)$. It is reasonable to allow flexibility in the description, because traffic flow is a self-driven, many-particle system that is very complex (Helbing, 2001), which means that a given choice for the pressure and equilibrium velocity might be suitable in one situation but not in another. More importantly, the mechanics of the LWR model should also be incorporated into the formulation, which is characterized by (or defined as) the equilibrium flow. However, there are no rigorous links between the anisotropic formulation and the LWR model. This discrepancy is undesirable because the higher-order models (including Eq. (3)) were developed to improve the LWR model. We remark that although traffic dynamics are well reflected by some of the aforementioned higher-order models, in which a metastable regime is supposed to reproduce stop-and-go waves, the LWR model can be successfully applied in many circumstances, such as near a bottleneck or in the vicinity of a traffic signal. The resultant equilibrium flow as derived by the LWR model, together with the shock and rarefaction waves, is frequently observed in reality.

Obviously, when describing real traffic there are advantages and disadvantages in using the LWR model for equilibrium flow and some of the higher-order models for non-equilibrium flow. The overall stable regime of the LWR model does not admit any “self-driven” increases in density that are known as “ghost jams” in observation. However, it does provide a dissipation mechanism (the rarefaction wave) that is able to describe the disappearance of a jam. In mathematical terms, the solution of the LWR model (as a standard scalar hyperbolic conservation equation) is nonlinearly stable in both TVD and L_∞ norms. In contrast, under a metastable regime (near the so-called congested density region) the higher-order models represent the evolution of an unstable density distribution into a stable (or unstable) jam, and offer a good explanation of the formation of the aforementioned ghost jams. However, these jams last forever and there underlines no mechanism for dissipation. Therefore, there is no compelling argument or evidence to preclude the use of any of these models to describe and explain complex traffic phenomena.

Based on the foregoing comments, we are motivated to establish a more general mathematical framework that includes both the LWR and higher-order models and in which both equilibrium and non-equilibrium traffic flows coexist in the traffic system, which is contrary to the nonreversible transition that is afforded by the existing higher-order models. Here, our model incorporates the mechanics, which are governed by the interaction between the functions $p(\rho)$ and $v_e(\rho)$, that may differ locationally, for example, with lane changing, on-and-off ramps, merging lanes, and traffic signals, or even temporally.

We now return to the foregoing discussion on the selection of a conserved variable for the acceleration equation, and argue that a new variable should be introduced. The coexistence of both equilibrium and non-equilibrium flows in the system suggests that the acceleration equation is consistent with the LWR model, in that there is a specific relation (which in the following is called the consistency condition) between the pressure p and equilibrium velocity v_e such that the acceleration equation is equivalent to Eq. (1) by setting $v = v_e(\rho)$. We stress that equivalence here refers to that in the distribution sense, which must hold both when the solution is smooth and when the solution is discontinuous. The consistency condition can easily be determined as $p'(\rho) = -v'_e(\rho)$ under the equivalence requirement for a smooth solution. To ensure the equivalence for a discontinuous solution, the conserved variable of the acceleration equation should essentially be identical to ρ (the conserved variable of Eq. (1)) under the same consistency condition. This suggests that the required conserved variable should essentially have a density dimension.

In Section 2, the mathematical framework for the discussed coexistent system is established. First, the required conserved variable is defined as a pseudo-density w that is derived from the transformation $v = v_{e1}(w)$ (*first regime*), where the function v_{e1} is actually a velocity–density relationship. Second, the pressure is defined as a function of w : $p(w) \equiv -v_{e2}(w)$ (*second regime*). This not only defines the required conservation form, but also reasonably reflects the influence of the velocity on the acceleration. These two relations inevitably result in an anisotropic formulation. Third, relaxation is achieved through the function $v_{e3}(\rho)$ (*third regime*), which takes into account the influence on acceleration of both the velocity and the density. The consistency conditions (with the LWR model) now become $v_{e1} = v_{e2} = v_{e3} \equiv v_e$.

In Section 3, physically bounded solution is thoroughly studied based on the characteristics theory. The isolines of the two characteristic variables in density–velocity coordinate plane are applied to confine the solution to a physically admissible region at large (**Proposition 1**). In particular, evolution of unstable equilibrium states is confined to a certain region properly (**Proposition 2**). This constitutes another contribution of the paper and can be easily extended to the study of higher-order traffic flow models in general. In Section 4, both equilibrium and non-equilibrium flows are simulated, and the analytical results are verified through numerical examples. A conclusion is offered in Section 5, with several issues being left for discussion in future studies.

2. Formulation of the model

In the formulation of the anisotropic traffic flow model, we introduce three conditions that influence the acceleration behavior of traffic. First, a new variable w is applied through the 1–1 transformation $v = v_{e1}(w)$, where v_{e1} is a function that is similar to a velocity–density relationship and satisfies the same properties as are in the LWR model, and thus $0 \leq w \leq \rho_{\text{jam}}$, where ρ_{jam} is the theoretical maximum density that can be defined as the reciprocal of the vehicle length. The variable w can be viewed as a desired density; or in terms of the car-following theory, $1/w$ represents a desired distance headway that is associated with the velocity v through the inverse function of v_{e1} , and that is usually smaller than the actual distance headway $1/\rho$ for safety consideration.

Second, we introduce a similar pressure p that is completely dependent on w (or v), rather than on density ρ . More precisely, p is a strictly decreasing function of v , and thus is a strictly increasing function of w , and is denoted by

$$p = p(v_{e1}(w)) \equiv p(w), \quad p'(w) > 0.$$

By translation, we assume that $p(\rho_{\text{jam}}) = 0$, and thus the function $-p(w)$, acts as a velocity–density relationship that is denoted by $v_{e2}(w) \equiv -p(w)$. Let us now imagine a flow under pressure $p = p(\rho)$ by adopting $v = v_{e2}(\rho)$ in the LWR model. Recall that the acceleration (Pipes, 1969) is

$$\frac{dv}{dt} = -\rho v'_{e2}(\rho) \frac{\partial v}{\partial x}.$$

We replace ρ in the foregoing equation with w to obtain an appropriate conservation form and to reflect both the equilibrium and non-equilibrium nature of the model, as indicated in a later discussion.

Third, we take into account the relaxation of the velocity v to a state $v_{e3}(\rho)$ with the relaxation time τ . Taking into account these three conditions, the acceleration equation can be written as

$$\partial_t v + (v + w v'_{e2}(w)) \partial_x v = \tau^{-1} (v_{e3}(\rho) - v). \quad (8)$$

Note that the convective part of Eq. (8) only involves v or w , and thus the term “velocity wave” is used. More significantly numerous conservation forms can be defined based only on Eq. (8). It is well known that different definitions result in different weak solutions because discontinuities can be hardly avoided, and it is thus necessary to determine a particular conservation form, which is sometimes called a balance equation, when relaxation source terms are involved. See Whitham (1974), Toro (1999) and LeVeque (2002), and a more relevant discussion in Zhang and Wong (2006).

We choose w as the conserved variable to relate the formulation to the LWR formulation such that (if desired) the solution from the former could be identical to or approaching that of the latter. This should occur for instances when the LWR model works well. Based on this novel idea, we replace v by $v_{e1}(w)$ in Eq. (8) and approximate the resultant $-\tau v'_{e1}(w) > 0$ by $v_{e1}(0)/\rho_{jam} \equiv \beta$. Thus, we obtain

$$\partial_t w + (v_{e1}(w) + w v'_{e2}(w)) \partial_x w = \beta^{-1} (v_{e1}(w) - v_{e3}(\rho)). \quad (9)$$

Furthermore, we denote

$$\varphi(w) = \int_0^w (v_{e1}(dw) + dw v'_{e2}(dw)), \quad R(\rho, w) = \beta^{-1} (v_{e1}(w) - v_{e3}(\rho)),$$

which, together with Eq. (1), gives the conservation system

$$\partial_t \rho + \partial_x (\rho v_{e1}(w)) = 0, \quad (10)$$

$$\partial_t w + \partial_x \varphi(w) = R(\rho, w). \quad (11)$$

Eqs. (10) and (11) can be rewritten in the vector form

$$u_t + f(u)_x = s(u), \quad (12)$$

with $u = (\rho, w)^T$, $f(u) = (\rho v_{e1}(w), \varphi(w))^T$, and $s(u) = (0, R(u))^T$, along with the Jacobian matrix and the two eigenvalues

$$f_u = \begin{bmatrix} v_{e1}(w) & \rho v'_{e1}(w) \\ 0 & \varphi'(w) \end{bmatrix}, \quad \lambda_1 = \varphi'(w) \leq \lambda_2 = v_{e1}(w) = v. \quad (13)$$

This clearly shows the anisotropic nature of the model. If $w \neq 0$, then $\lambda_1 < \lambda_2$, which means that the system is strictly hyperbolic, and the corresponding right eigenvectors are

$$p_1 = (\rho s v'_{e1}(w), w v'_{e2}(w))^T \quad \text{and} \quad p_2 = (1, 0)^T. \quad (14)$$

If $w = 0$, then $\lambda_1 = \lambda_2 = v_{e1}(0)$. Further, if $\rho = 0$, then the system is strongly hyperbolic, and p_1 and p_2 can be chosen as any two linearly independent vectors. This poses no problems mathematically. If $w = 0$ but $\rho > 0$, then the system is not strictly hyperbolic and the case should be avoided (see also the discussion in the end of Section 3.1).

In this paper, the model embodies the important idea that the physical properties of Eq. (12) are mostly related to the interaction among the three conditions or regimes. In principle, the traffic behavior will be very close to that which is described by the LWR model if the three conditions are in harmony. In contrast, if the three conditions are not in harmony, then the conflict among them may give rise to non-equilibrium flows with instabilities.

By a transformation $\bar{w} = \bar{w}(w)$, the convective parts of Eqs. (10) and (11) (or (9)) can become

$$\partial_t \rho + \partial_x (\rho V(\bar{w})), \quad \text{and} \quad \partial_t \bar{w} + \partial_x (\bar{w} V(\bar{w})),$$

where the function $V(\bar{w}) = v_{e1}(\bar{w}^{-1}(\bar{w})) = v$ is monotonically decreasing of \bar{w} . Actually, \bar{w} can be determined as

$$\bar{w} = \exp \left(\int_1^w \frac{v'_{e1}(dw)}{v'_{e2}(dw) w} \right),$$

with $0 \leq \bar{w} \leq \rho_{jam}$. This actually incorporates the two functions v_{e1} and v_{e2} into one by using the variable \bar{w} that is essentially the same as w . In other words, the transformation is essentially equivalent to setting $v_{e1} = v_{e2} \equiv V$ in Eqs. (10) and (11). However, we note that the transformation $\bar{w} = \bar{w}(w)$ is valid only for solution in smooth regions; it is invalid generally at the discontinuity. This implies that the claimed first and second regimes are intrinsically related to the conservation form of Eq. (11), or the discontinuity speed that is assumed to be determined accordingly.

The forthcoming discussion will be limited to the simple case for $v_{e1} = v_{e2} \equiv V$ in Eq. (11). However, the conclusions in Sections 3.1 and 3.2 only involve characteristic equations that are independent of the conservation form of Eq. (11), and thus are also applicable to the general case $v_{e1} \neq v_{e2}$ using a similar procedure. For the discussion of discontinuous solution in higher-order traffic flow models, we refer the interested readers to Zhang and Wong (2006) and Xu et al. (2007).

3. Solution properties and numerical scheme

As assumed, we replace the functions v_{e1} and v_{e2} by V , and re-denote the function v_{e3} by v_e . Thus, system (10) and (11) can be rewritten as

$$\partial_t \rho + \partial_x(\rho V(w)) = 0, \quad (15)$$

$$\partial_t w + \partial_x(wV(w)) = \beta^{-1}(V(w) - v_e(\rho)). \quad (16)$$

Here, we note that Eq. (16) can be written as the following transport form:

$$\partial_t(\rho z) + \partial_x(\rho z v) = \beta^{-1}(V(\rho z) - v_e(\rho)), \quad (17)$$

where $z = w/\rho$, and the transported variable ρz is analogous to the momentum in the Euler equations.

We also note that the convective part of Eq. (17) takes the same form as that of Eq. (7). Here, the variable $z = w/\rho$ is compared to $I = v - V(\rho)$ that was explained as the relative velocity to $V(\rho)$ in the ARZ model (Lebacque et al., 2007a) or the EARZ model (Lebacque et al., 2007b). Because we have the relation $I = v - V(\rho) = V(w) - V(\rho) \approx V'(\rho)\rho(z-1)$, by which $I \leq 0$ is equivalent to $z \geq 1$, the variable z also measures the deviation of the actual velocity v from $V(\rho)$. We remark that our conclusions in this section can be easily extended to Eq. (7) generally for $I = I(\rho, v)$.

It is obvious that Eq. (16) has already been a characteristic equation with the characteristic variable w (or $v = V(w)$) and corresponding to the characteristic speed $\lambda_1 = (wV(w))'$. By the transport form of Eq. (17) (together with Eq. (15)), z must be a characteristic variable corresponding to the characteristic speed $\lambda_2 = V(w)$, which easily suggests the other characteristic equation:

$$\partial_t z + \lambda_2 \partial_x z = z(\beta w)^{-1}(V(w) - v_e(w/z)), \quad \lambda_2 = V(w).$$

Accordingly, we define two families of characteristics together with solution equations in these characteristics, which constitute two systems of ordinary differential equations (ODE)

$$1\text{-field} : \quad \frac{dx}{dt} = \lambda_1, \quad \frac{dw}{dt} = \beta^{-1}(V(w) - v_e(w/z)); \quad (18)$$

$$2\text{-field} : \quad \frac{dx}{dt} = \lambda_2, \quad \frac{dz}{dt} = z(\beta w)^{-1}(V(w) - v_e(w/z)). \quad (19)$$

See Lebacque et al. (2007a,b), in which more details were presented for the derivation of the characteristic variables or equations for a transport equation similar to Eq. (17).

Although Eqs. (18) and (19) cannot be explicitly solved in general, they do well interpret physical meanings of wave propagation in traffic and serve for better understanding of mathematical properties of the solution.

3.1. Physically bounded solutions in general

Assume a certain vehicle in motion. Then, its influence is firstly through the 2-characteristic propagation (Eq. (19)) that synchronizes with the driving action ($\lambda_2 = v$). Here, changes of z in the propagation can be explained as the driver's adjustment to the surroundings, which depends on the local density $\rho = w/z$ through the relaxation. Furthermore, the driver's adjustment causes changes in w or $v = V(w)$, which actually serves as a velocity signal to propagate backwards through a 1-characteristic curve and with the relative speed $wV'(w) = \lambda_1 - v < 0$ (Eq. (18)), and thus influences the following vehicles.

Here, the ratio $z = w/\rho$ measures the deviation of some ideally allowed density w (or headway $1/w$) from the actual vehicular density ρ (or headway $1/\rho$). The equality $z = 1$ (or equivalently $v = V(\rho)$) represents "ideal" phase states. However, we assume that these desired states could hardly be reached by most drivers for safety or other reasons. In other words, we anticipate $z > 1$ or $v < V(\rho)$ generally in real traffic flows. Thus, $z = 1$ or $v = V(\rho)$ should be a boundary curve in density-velocity coordinate plane and be taken from approximately the maximum of the observed data. This should be true empirically for traffic flow in congestion or jamming. According to the argument below Eq. (14), this should also be true mathematically for sufficiently light traffic state, such that $V_f \equiv V(0) \geq v_f \equiv v_e(0)$. Otherwise, if $V_f < v_f$, the system would be non-strictly hyperbolic in these phase states (ρ, V_f) with $w = 0$ and for $\rho > 0$.

In Fig. 1, $V(\rho)$ is simply taken as a linear function for illustration purpose. With the increase of z , we can derive a family of curves $v = V(z\rho)$ in the figure, which are isolines of the deviation z ; in particular, $z = \infty$ coincides with the boundary $\rho = 0$. This argument implies that $z > 1$ and $z < 1$ hold, respectively beneath and above the curve $v = V(\rho)$. The isolines of w would be parallel straight lines starting decreasingly from $w = \rho_{\text{jam}}$ (corresponding to $v = V(\rho_{\text{jam}}) = 0$) to $w = 0$ (corresponding to $v = V(0) = V_f$). Referring to the isoline of z and the isoline of w (or equivalently the isoline of v), we give the following proposition, which implies that the model is free of collision and avoids reverse flow.

Proposition 1. Assume that $v_e(\rho) \leq V(\rho)$ and given the domain

$$D_1 = \{(\rho, v) | 1 < z < \infty, w < \rho_{\text{jam}}\}.$$

If the initial states are within D_1 , then the solution state (ρ, v) will be also bounded in D_1 .

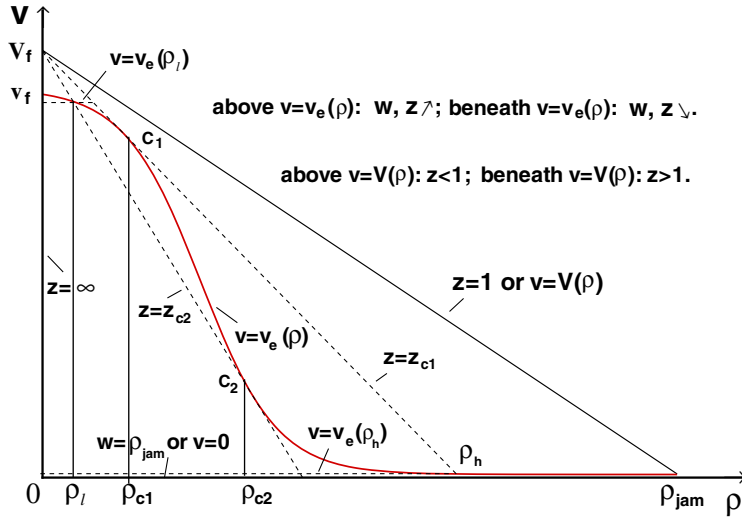


Fig. 1. Illustration of the physically bounded solution by isolines of two-characteristic variables z and w (or v). By Proposition 1, the solution is generally bounded by the isolines $z = 1$, $z = \infty$, and $v = 0$. By Proposition 2, the solution is particularly bounded by the isolines $z = z_{c_1}$, $z = z_{c_2}$, $v = v_e(\rho_l)$, and $v = v_e(\rho_h)$, which are related to the critical densities.

Proposition 1 can be easily indicated through propagations of the two characteristic fields. Let the trajectory $w = w(t)$ of Eq. (18) and the trajectory $z = z(t)$ of Eq. (19) in ρ - v coordinate plane be also called 1-characteristic curve and 2-characteristic curve, respectively. Then, according to the characteristic theory, we basically assume that each solution state (including those at discontinuities) is the intersection of a 1-characteristic curve and a 2-characteristic curve each of which starts from an initial state continuously. By Eq. (18), we claim that a 1-characteristic curve can never reach the border $w = \rho_{\text{jam}}$, because w is decreasing when traveling in the region that is beneath the curve $v = v_e(\rho)$. Here, the isolines of w are referred to. By Eq. (19), we claim that a 2-characteristic curve can never reach the border $z = 1$, because z is increasing when traveling in the region that is above the curve $v = v_e(\rho)$. Here, the isolines $v = V(z\rho)$ that increase from $z = 1$ to $z = \infty$ are referred to. Furthermore, a 2-characteristic curve can never reach the isoline $z = \infty$. We therefore conclude that any (ρ, v) in the borders can never be a solution state. Otherwise, some (ρ, v) in a border would be intersected by a 1-characteristic curve and a 2-characteristic curve, which in any case would be contradictory to at least one claim in the above. We also conclude that there is no solution states outside the region D because of the continuity of characteristics.

3.2. Physically bounded solutions related to stability conditions

The forthcoming discussion is concerned with the stability and instability of the equilibrium solution $(\rho, v) = (\rho_0, v_e(\rho_0))$, which are often responsible for the occurrence of stop-and-go waves or more complex waves observed in traffic flows.

According to Whitham (1974), this equilibrium is linearly stable if and only if its kinetic wave speed $(\rho v_e(\rho))'|_{\rho=\rho_0} = v_e(\rho_0) + \rho_0 v_e'(\rho_0)$ is between its two characteristic speeds $\lambda_1 = v_e(\rho_0)$ and $\lambda_2 = V(w_0) + w_0 V'(w_0)$. Here, w_0 is the function of ρ_0 that is implicitly determined by $V(w_0) = v_e(\rho_0)$, by which $dw_0/d\rho_0 = v_e'(\rho_0)/V'(w_0)$ is implied. The linear stability conditions turn out to be

$$\frac{dw_0}{d\rho_0} \leq \frac{w_0}{\rho_0} \equiv z_0, \quad \text{with } V(w_0) = v_e(\rho_0) \quad \text{or} \quad \frac{dz_0}{d\rho_0} \leq 0, \quad \text{with } V(z_0\rho_0) = v_e(\rho_0), \quad (20)$$

which can be interpreted through Fig. 1.

Actually, the equilibrium $v_0 \equiv v_e(\rho_0)$ traverses those isolines $v = V(z_0\rho)$ with z_0 non-increasing in a stable interval of ρ_0 when ρ_0 increases and (ρ_0, v_0) moves along the curve $v = v_e(\rho)$. An unstable interval of ρ_0 is implied if z_0 is increasing in this movement. A critical density $\rho_0 = \rho_c$ together with $z_0 = z_c$ can be solved by taking the equality of Eq. (20), which yields $V(z_0\rho_0) = v_e(\rho_0)$ and $dV(z_0\rho_0)/d\rho_0 = dv_e(\rho_0)/d\rho_0$ at $(\rho_0, z_0) \equiv (\rho_c, z_c)$. This suggests that $(\rho_c, v_e(\rho_c))$ is a tangent point of the equilibrium curve $v = v_e(\rho)$ and the isoline $v = V(z\rho)$. Two critical densities $\rho = \rho_{c_1}$ and $\rho = \rho_{c_2}$ are marked in Fig. 1, which show that the equilibrium solution $\rho = \rho_0$ is linearly unstable in a congested interval (ρ_{c_1}, ρ_{c_2}) and stable in other two intervals.

The density at the intersection of the isoline $v = V(z_{c_1}\rho)$ (or $z = z_{c_1}$) and the equilibrium curve $v = v_e(\rho)$ is marked by $\rho = \rho_h$, and the intersection of the isoline $v = V(z_{c_2}\rho)$ (or $z = z_{c_2}$) and the equilibrium curve $v = v_e(\rho)$ is marked by $\rho = \rho_l$. These serve as two important parameters and are shown in Fig. 1. We casually mention that if the initial states are within the region bounded by the isolines: $z = \infty$, $w = V^{-1}(v_e(\rho_h))$ and $z = z_{c_1}$, then all solution states will be confined

to the same region. Here V^{-1} denotes the inverse function of V , and the isoline $w = V^{-1}(\nu_e(\rho_h))$ can be also denoted by $\nu = \nu_e(\rho_h)$ as shown in Fig. 1. It would be similar to the foregoing discussion that supports this argument.

If more isolines are considered, we can also derive the bounded solution in several other regions similarly. However, this leads to more complicated issues which would be left for our future study. Nevertheless, it is significant to also consider the isoline $w = V^{-1}(\nu_e(\rho_l))$ (or $\nu = \nu_e(\rho_l)$ denoted in Fig. 1) and give the following proposition.

Proposition 2. Assume that $\nu_e(\rho) \leq V(\rho)$ and given the domain:

$$D_2 = \{(\rho, \nu) | z_{c_1} < z < z_{c_2}, \nu_e(\rho_h) < \nu < \nu_e(\rho_l)\}.$$

If the initial states are in D_2 , then the solution state (ρ, ν) will be also bounded in D_2 .

Proposition 2 can be easily indicated, which is similar to that for the discussion of **Proposition 1**. Here, we only note that a 1-characteristic curve cannot reach (probably can approach very closely) the isolines $\nu = \nu_e(\rho_l)$ and $\nu = \nu_e(\rho_h)$, and that a 2-characteristic curve cannot reach (probably can approach very closely) the isolines $z = z_{c_1}$ and $z = z_{c_2}$. By **Proposition 2**, we note that ρ_l and ρ_h are two density limits which cannot be exceeded during the evolution of solution in D_2 . More significantly, **Proposition 2** implies that evolution of an unstable equilibrium $\rho = \rho_0$ will be confined to the region D_2 , if the perturbed state is not large enough to exceed the boundary ∂D_2 .

Finally, we indicate that the solution of the model converges to that of the LWR model if setting $V(\rho) \equiv \nu_e(\rho)$. Assume that a solution at (x, t) is reached by a 2-characteristic curve from $x(0) = \eta$ with $w(\eta, 0) = w_0(\eta)$, and let recall $\beta = -\tau\nu'(w)$ and approximate $\nu_e(w) - \nu_e(w/z) = \nu'(w)(w - w/z)$. Then, the relaxation term of Eq. (16) becomes

$$\tau^{-1}(\rho - w), \quad (21)$$

and the deviation $z = w/\rho$ of Eq. (19) can be explicitly solved

$$z = 1 + (z_0(\eta) - 1)e^{-t/\tau}.$$

This verifies that $\rho \rightarrow w$ and $\nu \rightarrow \nu_e(\rho)$ for $t \rightarrow \infty$, by which the relaxation term vanishes and Eqs. (15) and (16) become identical with $V(w) = \nu_e(\rho)$. In this case, Eq. (20) always holds with $z_0 \equiv 1$.

3.3. Computational scheme

By applying Eq. (12), the first-order conservative scheme of system (15) and (16) is written as (Toro, 1999; LeVeque, 2002)

$$u_i^{n+1} = u_i^n - \frac{\Delta t}{\Delta x} \left(\hat{f}(u_i^n, u_{i+1}^n) - \hat{f}(u_{i-1}^n, u_i^n) \right) + s(u_i^n).$$

Here, the computation interval $(0, L)$ is divided into $K + 1$ cells with $i = 0, \dots, K + 1$, and $\hat{f} = (\hat{f}_1, \hat{f}_2)^T$ is the numerical flux function approximating the flux function $f = (f_1, f_2)^T$ with the components $f_1 = \rho V(w)$, and $f_2 = wV(w)$. For numerical stability, we generally set the CFL condition $\Delta t \leq \Delta x/V_f$, which means that the maximal characteristic speed V_f cannot exceed the cell speed $\Delta x/\Delta t$. We always take the equality of the CFL condition in the numerical simulation.

In designing the Godunov scheme, the function $\hat{f}(u_1, u_2)$ is acquired from the exact flux value in the interface $x = 0$, by solving the homogeneous model equations (derived by setting $s(u) = 0$ in (12)) with the Riemann data: $u(x, 0) = u_1$ for $x < 0$; $u(x, 0) = u_2$ for $x > 0$. This suggests the denotation of the self-similarity solution $u(x, t) = u(x/t)$ and the function $\hat{f}(u_1, u_2) = f(u(0))$. See Lebacque et al. (2007a,b) for detailed discussion for the relevant problem. We can similarly derive

$$\hat{f}_2^G(u_1, u_2) = \begin{cases} \min_{w_1 \leq w \leq w_2} f_2(w), & \text{if } w_1 \leq w_2, \\ \max_{w_1 \geq w \geq w_2} f_2(w), & \text{if } w_1 > w_2, \end{cases} \quad \hat{f}_1^G(u_1, u_2) = \frac{\rho_1}{w_1} \hat{f}_2^G(u_1, u_2).$$

Here, $\hat{f}_2^G(u_1, u_2) = \hat{f}(w_1, w_2)$ is actually the well known Godunov flux (Cockburn, 1997; Shu, 1998), which approximates $f_2(w)$ in solving the homogeneous equation of (16) separately. The numerical flux \hat{f}_1^G is derived from the identity $f_1(u(0)) = f_2(u(0))\rho(0)/w(0)$ with $w(0)/\rho(0) = w_1/\rho_1$. The latter equality holds because the characteristic variable $z = w/\rho$ as a Riemann invariant can always reach the interface $x = 0$ when traveling from the left-hand side with $z = w_1/\rho_1$. Because of the transport form of Eq. (17), this argument remains true even for the occurrence when z travels across a 1-shock.

For an initial value problem, the computation proceeds with $(x, t) \in [0, L] \times [0, T]$, such that the two boundaries $x = 0$ and $x = L$ fall into smooth regions and $u(0, t)$ and $u(L, t)$ satisfy the system. Replacing u by $u(0, t)$ and $u(L, t)$ in Eqs. (15) and (16) gives, by discretization

$$\begin{aligned} \rho_0^{n+1} &= \rho_0^n, & w_0^{n+1} &= w_0^n - \Delta t(\nu_e(\rho_0^n) - V(w_0^n))/\beta, \\ \rho_{K+1}^{n+1} &= \rho_{K+1}^n, & w_{K+1}^{n+1} &= w_{K+1}^n - \Delta t(\nu_e(\rho_{K+1}^n) - V(w_{K+1}^n))/\beta. \end{aligned}$$

These boundary values are actually acquired from the parallel propagation of the characteristics, and in the computation are identified by the constant ρ (Zhang et al., 2005). The periodic boundary conditions

$$\rho_0^n = \rho_K^n, \quad \rho_{K+1}^n = \rho_1^n; \quad w_0^n = w_K^n, \quad w_{K+1}^n = w_1^n,$$

are also applied in numerical simulation.

We note that $v(x, 0)$ should be properly given for a zero initial density. If it is supposed that $\rho(x, 0) = 0$ for $x \in (x_1, x_2)$, then it is physically sound to define

$$v(x, 0) = v(x_1, 0), \quad \text{for } x \in (x_1, x_2), \quad (22)$$

where $x = x_1$ represents the leading vehicle in a queue that is not influenced by the waves from $x \geq x_2$ and accelerates only by relaxation until it catches up (if possible) with the vehicle that is initially at location $x = x_2$. The initial state of $\rho(x_1, 0) = 0$ and $v = v(x_1, 0)$ at $x_1 = -\infty$ is assumed to be in equilibrium with $v(x_1, 0) = v_e(0) = v_f$.

4. Simulation of traffic phenomena

Different forms of the functions $v_e(\rho)$ and $V(\rho)$ are selected so that the simulation results are shown to reproduce some observed traffic flow phenomena under different circumstances. In the following, we present a few examples, which combine with the discussion in Section 3, should be conducive to further study of the traffic flow theory. The choice of the functions $V(\rho)$ and $v_e(\rho)$ and the parameters therein can be calibrated from field data (see e.g., Beskos et al., 1984; Lyrintzis et al., 1994). In the numerical simulations, all of the results are shown by dimensionless variables, for which L , ρ_{jam} , V_f , and T are scaled to unity. In general, they are assumed whenever they are not followed by a unit.

4.1. Equilibrium flow

For the simulation of equilibrium flow, we set $v_e \equiv V$ and replace the relaxation term in Eq. (16) by Eq. (21). The function $V(\rho)$ is given by (Del Castillo and Benitez, 1995a,b)

$$V(\rho) = V_f \left[1 - \exp \left(1 - \exp \left(\frac{c_0}{V_f} (\rho_{\text{jam}}/\rho - 1) \right) \right) \right]. \quad (23)$$

In numerical simulation, we assume the following constant parameters:

$$L = 2000 \text{ m}, \quad \Delta x = 5 \text{ m}, \quad V_f = 20 \text{ s/m}, \quad c_0/v_f = 0.3, \quad \tau = 10 \text{ s}, \quad \rho_{\text{jam}} = 0.16 \text{ veh./m},$$

and the density ρ in Eq. (23) is replaced by $\rho + \epsilon \rho_{\text{jam}}$ with $\epsilon = 10^{-6}$ in order to avoid appearance of 0 in the denominator. We note that the corresponding flow function $Q(\rho) \equiv \rho V(\rho)$ of Eq. (23) is strictly concave with $Q''(\rho) < 0$.

In Fig. 2, the density change that is caused by a traffic signal is shown with a simulation time of $T = 60$ s:30 s of red¹ signal followed by 30 s of green signal. The initial data are given by $\rho(x, 0) = 0.2$, and $v(x, 0) = 0.7$ for $x > 0.01$; and $\rho(x, 0) = 0$, and $v(x, 0) = v_f$ otherwise. The simulation begins with the red signal, which is described as an extra boundary condition at the crossing $x = 0.25$, namely, we set $v(0.25, t) = 0$ for $t < 30$ s. When the signal changes to green at $t = 30$ s, the computation continues as for the initial problem and $v(x, 30)$ is re-defined following the rule of Eq. (22).

In Fig. 3, we show a more complex traffic situation. Applying similar techniques, the traffic near a toll-gate is also simulated for $T = 60$ s. Initially, $\rho(x, 0) = 0.2$, and $v(x, 0) = 0.7$ for $x < 0.2$; and $\rho(x, 0) = 0$, and $v(x, 0) = 0$ otherwise. At the toll-gate $x = 0.2$, we set the extra boundary condition $v(0.2, t) = 0$ for $t - 6[t/6] \leq 1$ s, which means a 1 s stop for payment every 6 s.

These two examples reasonably reproduce the jamming and dissipation through the application of the variable v (or w) as a switch function at appropriate locations.

4.2. Non-equilibrium flow with two critical densities

As suggested in the foregoing discussions, we adopt a function $v_e(\rho) \neq V(\rho)$ to simulate the non-equilibrium flow. With $V(\rho)$ given by Eq. (23) and $v_e(\rho)$ given by Kerner and Konhäuser (1994)

$$v_e(\rho) = v_f \left\{ \left[1 + \exp \left(\frac{\rho/\rho_{\text{jam}} - 0.25}{0.06} \right) \right]^{-1} - 3.72 \times 10^{-6} \right\}, \quad (24)$$

$v_e(\rho) \leq V(\rho)$ holds and thus Propositions 1 and 2 are applicable. For $V_f = v_f$ and a range of values of c_0/V_f , we solve two critical densities ρ_{c_1} and ρ_{c_2} from Eq. (20), which along with several other corresponding parameters are listed in Table 1. In numerical simulation, we apply the following constants:

$$L = 16,000 \text{ m}, \quad \Delta x = 10 \text{ m}, \quad v_f = 25 \text{ s/m}, \quad \tau = 30 \text{ s}. \quad (25)$$

For $c_0/v_f = 0.2$, we redraw several reference curves of Fig. 1 in the q - ρ coordinate through the relation $q = \rho v$. Accordingly, the flow function $q_e = \rho v_e(\rho)$ corresponding to $v = v_e(\rho)$, and the isolines $z = z_1$, $z = z_2$, and $v = v_e(\rho_h)$ are now defined by $q = \rho V(z_1 \rho)$, $q = \rho V(z_2 \rho)$, and $q = \rho v_e(\rho_h)$. These curves are shown in Fig. 4. The isoline $v = v_e(\rho_l)$ is not shown, because it as a boundary of D_2 now reduces to the origin $(0, 0)$ with $\rho_l = 0$ under the condition $V_f = v_f$.

¹ For interpretation of color in Figs. 2 and 4, the reader is referred to the web version of this article.

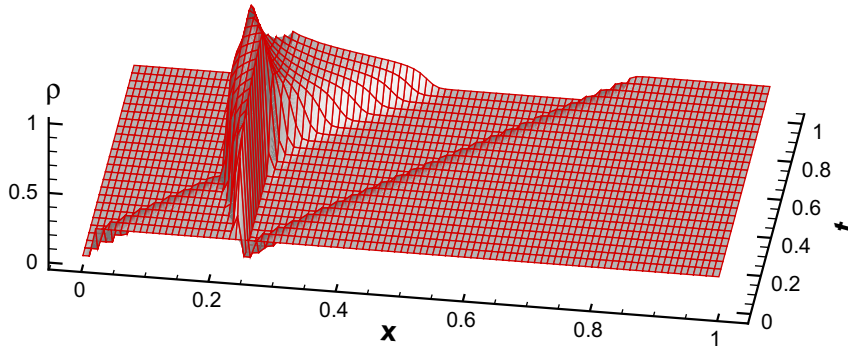


Fig. 2. Change in density at a traffic signal with 30 s red light and 30 s green light.

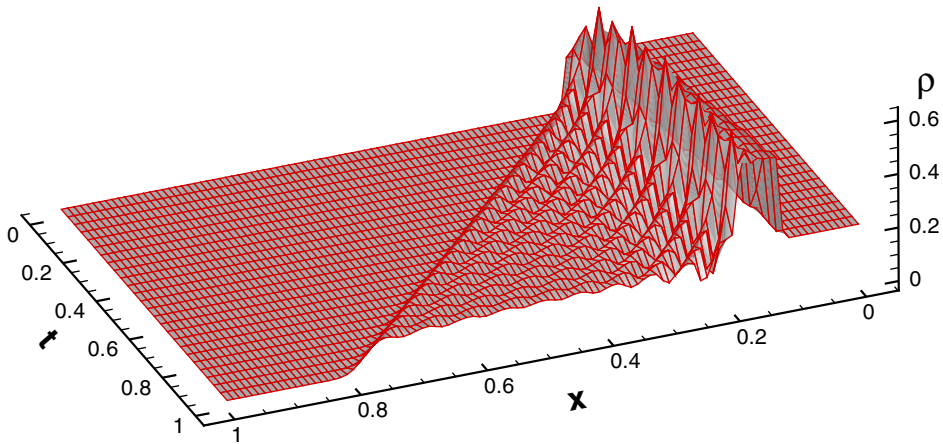


Fig. 3. Change in density near a toll-gate that arises from a 1 s stop every 6 s for payment, which gives rise to congestion upstream and fluctuation downstream.

Table 1

Two critical densities ρ_{c_1} and ρ_{c_2} solved by taking the equality of Eq. (20) for different $V(\rho)$.

$V(\rho)$ given by Eq. (23)				$V(\rho)$ given by Eq. (27)			
c_0/V_f	0.20	0.25	0.30	α	0.5	0.75	1.0
ρ_{c_1}	0.19337	0.19788	0.20250	ρ_{c_1}	NE	NE	0.0
ρ_{c_2}	0.45564	0.43818	0.42334	ρ_{c_2}	0.40088	0.36832	0.34308
z_{c_1}	1.01313	1.20663	1.38123	z_{c_1}	NE	NE	0.67346
z_{c_2}	1.89646	1.95631	2.00910	z_{c_2}	2.13512	2.28203	2.40500
ρ_{jam}	0.98704	0.82875	0.72400	ρ_{jam}	1.0	1.0	1.0

NE: Not exist.

For numerical experiment, we apply the initial data:

$$\rho(x, 0) = \begin{cases} \rho_1, & \text{if } x \in [0, 0.65], \\ \rho_2, & \text{if } x \in (0.65, 0.85), v(x, 0) = v_e(\rho(x, 0)), \\ \rho_3, & \text{if } x \in (0.85, 1), \end{cases} \quad (26)$$

which represent three unstable equilibria by setting ρ_1 , ρ_2 and ρ_3 all between ρ_{c_1} and ρ_{c_2} . Thus, the evolved solution states are all expected to fall into the region bounded by $z = z_1$, $z = z_2$, and $v = v_e(\rho_h)$. This is according to [Proposition 2](#). Assuming three sets of data: (i) $(\rho_1, \rho_2, \rho_3) = (0.2, 0.21, 0.22)$, (ii) $(\rho_1, \rho_2, \rho_3) = (0.3, 0.31, 0.32)$, and (iii) $(\rho_1, \rho_2, \rho_3) = (0.4, 0.41, 0.42)$, and applying the periodic boundary conditions, we simulate for $t = 1800$ s and record $(\rho(x, t), q(x, t))$ every 30 s in the locations at every 80 m. These phase states are shown in [Fig. 4](#), which are all bounded in the region D_2 . This confirms the anticipation by [Proposition 2](#).

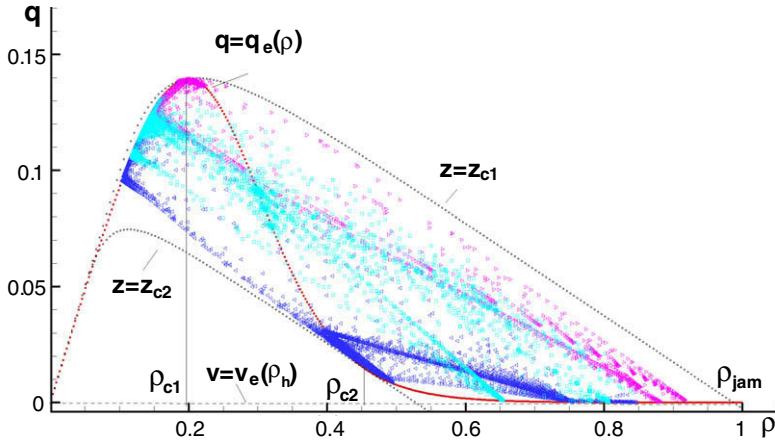


Fig. 4. Scattered phase points which are bounded by D_2 as is predicted by Proposition 1, and which indicate that a higher average density generally results in a lower flow rate in a highway section.

While the phase points of set (ii) (with cyan and square symbols) scatter mainly in the middle, the phase points of sets (i) (with purple and right triangle symbols) and (iii) (with blue and left triangle symbols) scatter, respectively in the upper and lower parts of the region. This indicates a decreasing average flow rate from (i) to (iii), with an increase in the average initial density. We note that the average density in the computation interval remains constant for application of the periodic boundary conditions. The numerical results reasonably suggest that a higher average density should generally give rise to a less efficient traffic flow.

Setting different densities of three unstable equilibria in Eq. (26) serves as perturbations for waves at locations $x = 0.65$, $x = 0.85$ and $x = 1$. Fig. 5 shows the development of these waves in 1600 s for set (ii). From the figure, we see that these waves evolve into congestion and jams that propagate backwards, known as stop-and-go waves. For longer time of evolution, the experiment indicates that a stable wide cluster (traveling wave) solution is derived. This is also the case for sets (i) and (iii), and the derived wide clusters have the deterministic maximal and minimal densities, and thus a fixed traveling speed. We refer the reader to a recent work by Zhang and Wong (2006), in which a analytical tool was proposed to determine the parameters of a wide cluster solution in higher-order models.

4.3. Non-equilibrium flow with one critical density

Let $v_e(\rho)$ be given by Eq. (24), and $V(\rho)$ by

$$V(\rho) = V_f \left(1 - \left(\frac{\rho}{\rho_{\text{jam}}} \right)^\alpha \right). \quad (27)$$

We again set $V_f = v_f$, such that V_f moves to coincide with v_f in Fig. 1, where the curve $v = v_e(\rho)$ is drawn actually according to Eq. (24). Then, for $\alpha = 1$, the straight line $v = V(\rho)$ is expected to intersect with $v = v_e(\rho)$. For $\alpha < 1$, the curve $v = V(\rho)$

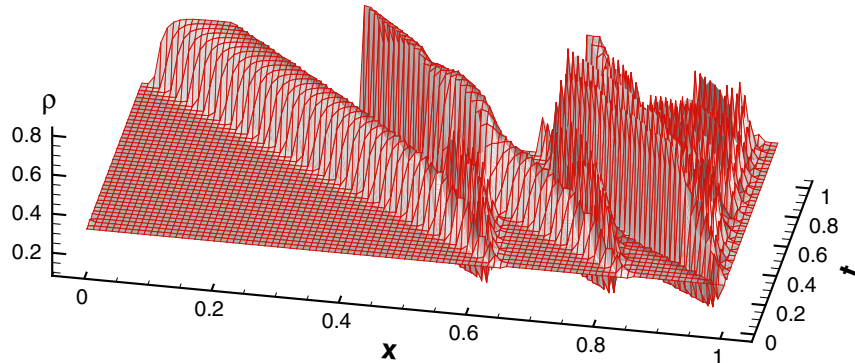


Fig. 5. Evolution of congestion and jams in 1600 s from unstable initial equilibrium distribution for set (ii), which is expected to evolve into a regular cluster for $t \rightarrow \infty$.

becomes even lower and still intersect with $v = v_e(\rho)$. This violates the assumption $v_e(\rho) \leq V(\rho)$ in the lower density region but still ensures the system to be strictly hyperbolic (see the discussions below Eq. (14) and in the second paragraph of Section 3.1). Although there is no analytical conclusion for bounded solution for such cases, invalid phase states are unlikely to develop for cautious choices of parameters because phase characteristics would approach the equilibrium curve $v = v_e(\rho)$ with exponential rate through relaxation.

The above setting is novel in that there exists only one critical density ρ_{c_2} , whereas ρ_{c_1} is identical to 0 (for $\alpha = 1$) or does not exist (for $\alpha < 1$). In this case, the parameter z_{c_1} does not exist and the jam density can be simply defined as $\rho_h = \rho_{jam}$. For a set of values $\alpha \leq 1$, the critical density ρ_{c_2} together with the related parameters are also indicated in Table 1. The description implies that equilibria in lower density region are still unstable, which differs from most existing theories. However, we remark that this result seems reasonable in a microscopic view, in that the density and flow could hardly remain constant even for very light traffic. A similar instance was also found in the Aw and Rascle model (2000) recently by Xu et al. (2007).

The periodic boundary conditions and the same constants of Eq. (25) are applied. Assume the following initial distribution (Kerner and Konhäuser, 1994)

$$\rho(x, 0) = \rho_0 + \Delta\rho_0 \left\{ \cosh^{-2} \left[\frac{160}{L} \left(x - \frac{3L}{8} \right) \right] - \frac{1}{4} \cosh^{-2} \left[\frac{40}{L} \left(x - \frac{13L}{32} \right) \right] \right\},$$

where $v(x, 0) = v_e(\rho(x, 0))$, and the second term acts as a local perturbation to the unstable constant distribution $\rho(x, 0) = \rho_0 < \rho_{c_2}$. Fig. 6 shows the numerical results for the choice of $\alpha = 1$, $\rho_0 = 0.22$, and $\Delta\rho_0 = 0.2$.

In the vicinity of larger perturbation, a backward moving jam is observed (Fig. 6(a)), which is similar to the case when $V(\rho)$ is given by Eq. (23). Moreover, waves with fluctuation are developed, propagate downstream with increasing swings and decreasing speeds, and eventually evolve into the backward moving jam. This latter evolution differs from that observed in Fig. 5, in which case the local congestions can hardly propagate downstream because there is little space in the region D_2 for higher flow near the fluctuation around $\rho = 0.2$ (Fig. 4). In contrast, Fig. 6b shows much larger region and thus higher flow rate for the scattered phase states, which are bounded by the isoline $z = z_{c_2}$ and the curve of the “ideal” density–flow relation $q = \rho V(\rho) \equiv Q(\rho)$. By Fig. 6b, it seems that the solution could also be properly bounded for $v = V(\rho)$ being given by Eq. (27).

Finally, we select and show two observed stop-and-go waves in Fig. 6c. We note that they are very close to a traveling wave solution but are unstable for a longer evolution. This is mainly because these “free traffic” states outside the clusters are unstable. Actually, new waves will develop and increase in these free traffic states. On the other hand, we can observe stable wide cluster when setting a much smaller relaxation time, in which case the free traffic states converge to constant equilibrium flow very quickly, thus no new wave arises.

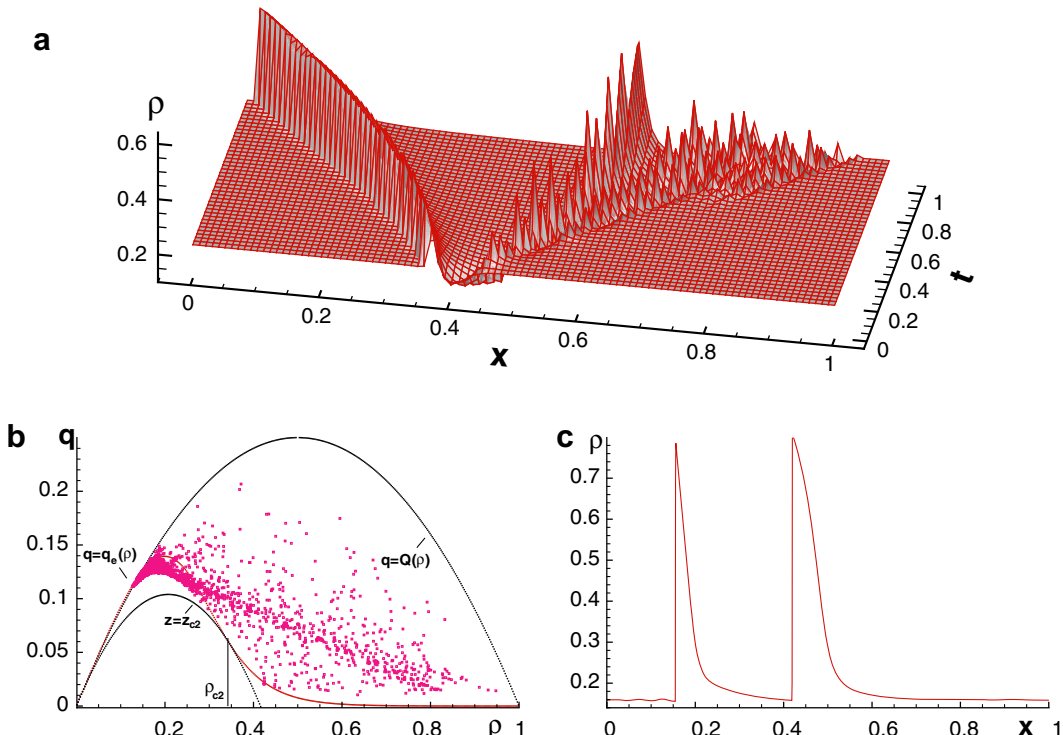


Fig. 6. Evolution of unstable initial equilibrium distribution, (a) congestion and jams in 750 s; (b) scattered phase points in 10,000 s, recorded every 200 s and at every 80 m; (c) two stop-and-go waves at $t = 5800$ s, which are not expected to evolve into stable clusters for $t \rightarrow \infty$.

5. Conclusion

We model anisotropic traffic flow by proposing three conditions. Through the characteristic variables, the traffic waves are physically interpreted, and the solution is verified to be properly bounded. More significantly, the bounded solution is related to traffic instability such that evolution of an unstable equilibrium is confined to a particular region in density–velocity or density–flow coordinate plane. The model is able to describe both equilibrium and non-equilibrium flows, which is indicated through numerical simulation of complex traffic phenomena. Numerical examples also indicate physically bounded solutions that agree with analytical results completely.

Future studies are suggested in the following areas.

- (a) The incorporation of inhomogeneous road conditions including locationally dependent functions v_{el} ($l = 1, 2, 3$) into the system of (10) and (11); see the related work in Zhang et al. (2005) and Bürger et al. (2008).
- (b) A promising extension of the model to traffic networks for the system of (10) and (11); see Holden and Risebro (1995), Coclite and Piccoli (2005), and Herty et al. (2006).
- (c) The development of a multi-class version of the model (which in general would be very challenging); see the related work in Wong and Wong (2002), Zhang et al. (2006), and Gupta and Katiyar (2007).
- (d) The development of high-order accurate numerical schemes; see Zhang et al. (2003), and Lu et al. (2008).

Acknowledgements

The work that is described in this paper was jointly supported by grants from the National Natural Science Foundation of China (70629001, 10771134, and 10532060), the National Basic Research Program of China (2006CB705500), and the Research Grants Council of the Hong Kong Special Administrative Region of China (Project No.: HKU7031/02E), the University of Hong Kong (10207394).

References

- Aw, A., Rascle, M., 2000. Resurrection of second order models of traffic flow. *SIAM Journal on Applied Mathematics* 60 (3), 916–938.
- Beskos, D.E., Okutani, I., Michalopoulos, P.G., 1984. Testing of dynamic models for signal controlled intersections. *Transportation Research Part B* 18 (4/5), 397–408.
- Bürger, R., Gracia, A., Karlsen, K.H., Towers, J.D., 2008. Difference schemes, entropy solutions, and speedup impulse for an inhomogeneous kinematic traffic flow model. *Networks and Heterogeneous Media* 3 (1), 1–41.
- Cockburn, B., 1997. Lecture Notes in Mathematics – An Introduction to the Discontinuous Galerkin Method for Convection-Dominated Problems [R]:1697. Springer, Cetraro, Italy, pp. 151–185.
- Coclite, G.M., Piccoli, B., 2005. Traffic flow on a road network. *SIAM Journal on Mathematical Analysis* 36 (6), 1862–1886.
- Daganzo, C.F., 1995. Requiem for second-order fluid approximations of traffic flow. *Transportation Research Part B* 29 (4), 277–286.
- Del Castillo, J.M., Benítez, F.G., 1995a. On the functional form of the speed–density relationship I: general theory. *Transportation Research Part B* 29 (5), 373–389.
- Del Castillo, J.M., Benítez, F.G., 1995b. On the functional form of the speed–density relationship II: empirical investigation. *Transportation Research Part B* 29 (5), 391–406.
- Greenberg, J.M., 2004. Congestion redux. *SIAM Journal on Applied Mathematics* 64 (4), 1175–1185.
- Gupta, A.K., Katiyar, V.K., 2007. A new multi-class continuum model for traffic flow. *Transportmetrica* 3 (1), 73–85.
- Helbing, D., 2001. Traffic and related self-driven many-particle systems. *Reviews of Modern Physics* 73 (4), 1067–1141.
- Herty, M., Moutari, S., Kirchener, C., 2006. Multi-class traffic models on road networks. *Communications in Mathematical Sciences* 4 (3), 591–608.
- Holden, H., Risebro, N.H., 1995. A mathematical model of traffic flow on a network of unidirectional roads. *SIAM Journal on Mathematical Analysis* 26 (4), 999–1017.
- Jiang, R., Wu, Q.S., Zhu, Z.J., 2002. A new continuum model for traffic flow and numerical tests. *Transportation Research Part B* 36 (5), 405–419.
- Kerner, B.S., Konhäuser, P., 1994. Structure and parameters of clusters in traffic flow. *Physical Review Part E* 50 (1), 54–83.
- Kühne, R.D., 1984. Macroscopic freeway model for dense traffic-stop-start waves and incident detection. In: Volmuller, J., Hamerslag, R. (Eds.), *Proceedings of the 9th International Symposium on Transportation and Traffic Theory*. VNU Science Press, Utrecht, pp. 21–42.
- Lebacque, J.P., Mammar, S., Haj-Salem, H., 2007a. The Aw-Rascle and Zhang's model: vacuum problems, existence and regularity of the solutions of the Riemann problem. *Transportation Research Part B* 41 (7), 710–721.
- Lebacque, J.P., Mammar, S., Haj-Salem, H., 2007b. Generic second order traffic flow modelling. In: Allsop, R.E., Bell, M.G.H., Heydecker, B.G. (Eds.), *Transportation and Traffic Theory*. Elsevier, London, pp. 755–776.
- LeVeque, R.J., 2002. *Finite Volume Methods for Hyperbolic Systems*. Cambridge University Press, New York.
- Lighthill, M.J., Whitham, G.B., 1955. On kinematic waves: II A theory of traffic flow on long crowded roads. *Proceedings of the Royal Society of London, Series A* 229 (1178), 317–345.
- Lu, Y., Wong, S.C., Zhang, M., Shu, C.W., Chen, W., 2008. Explicit construction of entropy solutions for the Lighthill–Whitham–Richards traffic flow model with a piecewise quadratic flow–density relationship. *Transportation Research Part B* 42 (4), 355–372.
- Lyrintzis, A.S., Yi, Ping, Michalopoulos, P.G., Beskos, D.E., 1994. Advanced continuum traffic flow models for congested freeways. *Journal of Transportation Engineering* 120 (3), 461–477.
- Payne, H.J., 1971. Models of freeway traffic and control. In: Bekey, A.G. (Ed.), *Mathematical Models of Public Systems Simulation Council Proceedings*, vol. 1. La Jolla, pp. 51–61.
- Pipes, L.A., 1969. Vehicle accelerations in the hydrodynamic theory of traffic flow. *Transportation Research* 3 (2), 229–234.
- Rascle, M., 2002. An improved macroscopic model of traffic flow: derivation and links with the Lighthill–Whitham model. *Mathematical and Computer Modelling* 35 (5/6), 581–590.
- Richards, P.I., 1956. Shockwaves on the highway. *Operations Research* 4 (1), 42–51.
- Shu, C.-W., 1998. Essentially non-oscillatory and weighted essentially non-oscillatory schemes for hyperbolic conservation laws. In: Cockburn, B., Johnson, C., Shu, C.-W., Tadmor, E. (Eds.), *Advanced Numerical Approximation of Nonlinear Hyperbolic Equations, Lecture Notes in Mathematics*, vol. 1697. Springer, pp. 325–432.

- Smoller, J., 1983. Shock Waves and Reaction-Diffusion Equations. Springer-Verlag, New York.
- Toro, E.F., 1999. Riemann Solvers and Numerical Methods for Fluid Dynamics. Springer, Berlin.
- Whitham, G.B., 1974. Linear and Nonlinear Waves. John Wiley and Sons, New York.
- Wong, G.C.K., Wong, S.C., 2002. A multi-class traffic flow model – an extension of LWR model with heterogeneous drivers. *Transportation Research Part A* 36 (9), 827–841.
- Xue, Y., Dai, S.Q., 2003. Continuum traffic model with the consideration of two delay time scales. *Physical Review Part E* 68 (6), 066123.
- Xu, R.Y., Zhang, P., Dai, S.Q., Wong, S.C., 2007. Admissibility of a wide cluster solution in anisotropic higher-order traffic flow models. *SIAM Journal on Applied Mathematics* 68 (2), 562–573.
- Zhang, H.M., 2002. A non-equilibrium traffic model devoid of gas-like behavior. *Transportation Research Part B* 36 (3), 275–290.
- Zhang, P., Wong, S.C., 2006. Essence of conservation forms in the traveling wave solutions of higher-order traffic flow models. *Physical Review Part E* 74 (2), 026109.
- Zhang, M., Shu, C.W., Wong, G.C.K., Wong, S.C., 2003. A weighted essentially non-oscillatory numerical scheme for a multi-class Lighthill–Whitham–Richards traffic flow model. *Journal of Computational Physics* 191 (2), 639–659.
- Zhang, P., Liu, R.X., Wong, S.C., 2005. High-resolution numerical approximation of traffic flow problems with variable lanes and free-flow velocities. *Physical Review Part E* 71 (5), 056704.
- Zhang, P., Liu, R.X., Wong, S.C., Dai, S.Q., 2006. Hyperbolicity and kinematic waves of a class of multi-population partial differential equations. *European Journal of Applied Mathematics* 17 (2), 171–200.